ACS APPLIED MATERIALS & INTERFACES

Research Article

www.acsami.org

Radiotherapeutic Bandage Based on Electrospun Polyacrylonitrile Containing Holmium-166 Iron Garnet Nanoparticles for the Treatment of Skin Cancer

Imalka Munaweera,[†] Daniel Levesque-Bishop,[†] Yi Shi,[‡] Anthony J. Di Pasqua,*[,‡] and Kenneth J. Balkus, Jr.*[,†]

[†]Department of Chemistry, University of Texas at Dallas, Richardson, 800 West Campbell Road, Richardson, Texas 75080, United States

[‡]Department of Pharmaceutical Sciences, University of North Texas System College of Pharmacy, University of North Texas Health Science Center, 3500 Camp Bowie Boulevard, Fort Worth, Texas 76107, United States

Supporting Information

ABSTRACT: Radiation therapy is used as a primary treatment for inoperable tumors and in patients that cannot or will not undergo surgery. Radioactive holmium-166 (^{166}Ho) is a viable candidate for use against skin cancer. Nonradioactive holmium-165 (^{165}Ho) iron garnet nanoparticles have been incorporated into a bandage, which, after neutron-activation to ^{166}Ho, can be applied to a tumor lesion. The ^{165}Ho iron garnet nanoparticles (^{165}HoIG) were synthesized and introduced into polyacrylonitrile (PAN) polymer solutions. The polymer solutions were then electrospun to produce flexible nonwoven bandages, which are stable to neutron-activation. The fiber mats were characterized using scanning electron microscopy, transmission electron microscopy, powder X-ray diffraction, Fourier transform infrared spectroscopy, thermogravimetric analysis and inductively coupled plasma mass spectrometry. The bandages are stable after neutron-activation at a thermal neutron-flux of approximately 3.5×10^{12} neutrons/cm^2·s for at least 4 h and 100 °C. Different amounts of radioactivity can be produced by changing the amount of the ^{165}HoIG nanoparticles inside the bandage and the duration of neutron-activation, which is important for different stages of skin cancer. Furthermore, the radioactive bandage can be easily manipulated to irradiate only the tumor site by cutting the bandage into specific shapes and sizes that cover the tumor prior to neutron-activation. Thus, exposure of healthy cells to high energy β-particles can be avoided. Moreover, there is no leakage of radioactive material after neutron activation, which is critical for safe handling by healthcare professionals treating skin cancer patients.

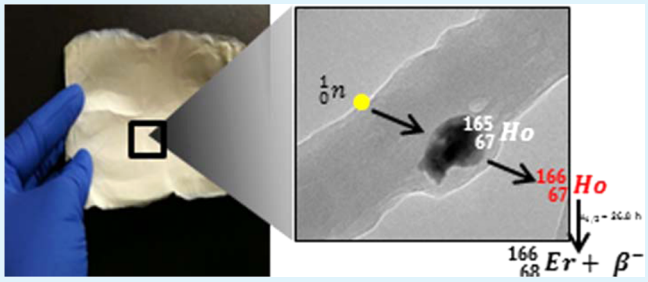

KEYWORDS: *cancer, radiotherapy, electrospinning, fibers, neutron-activation, skin cancer therapy, holmium-166*

INTRODUCTION

Cancer continues to gravely impact the health of society; thus, different methods are being sought and implemented to more efficiently and effectively combat this disease. Currently, it is estimated that one in every five Americans will develop skin cancer during their lifetime.[1] Chemo- and radiotherapy are currently used in the clinic to treat and manage cancer. External radiotherapy for skin cancer can be done using an electron beam,[2] X-rays[3] or a neutron beam.[4] Brachytherapy is another radiotherapeutic approach.[5] In radiotherapy, the cancer cell's DNA is damaged;[6] once the cancer cells are damaged, they can be eliminated from the body by the immune system.[7] We have developed bandages that contain radionuclides that can be applied externally on a patient's skin lesion for selective radiotherapy. Incorporating hazardous radionuclides in a carrier can be a challenge; the process must be amenable to large amounts of radioactivity and radionuclides with short half-lives. Neutron-activation can overcome this limitation by using stable isotopes such as holmium-165 (^{165}Ho), which can be neutron-activated to holmium-166 (^{166}Ho) after incorporation in a carrier. The emission of high energy β-particles with a maximum energy of 1.84 MeV and the relatively short half-life of 26.8 h make ^{166}Ho useful as a therapeutic radionuclide.[8] In addition, ^{166}Ho emits γ photons (6.6% photon yield), which can be used for quantifying and imaging.[8] ^{89}Y-containing TheraSphere can be neutron-activated to ^{90}Y (half-life of 64.2 h) and has been used to treat liver metastasis.[9] Holmium-165 is better than yttrium 89 because it has a short half-life and higher photon emission than yttrium.

Radioactive bandages/patches/films have been reported with various levels of success. Radiotherapeutic patches containing the radionuclides ^{165}Dy, ^{166}Ho, ^{32}P, ^{188}Re, ^{192}Ir and ^{90}Y coated on the surface of a paper or a polyethylene film, have been reported.[10−14] For example, Lee and co-workers prepared a

Received: September 4, 2014
Accepted: November 14, 2014
Published: November 14, 2014

Table 1. Composition of HoIG Nanoparticles Dispersed Polymer Solutions and Electrospinning Parameters

sample	PAN (g)	^{165}HoIG nanoparticles (g)	volume of DMF (mL)	rate (mL/h)	voltage (kV)	electrode separation distance (cm)
33% (w/w) ^{165}HoIG	1.0	0.5	10	0.05	14	6
50% (w/w) ^{165}HoIG	1.0	1.0	10	0.05	14	6

^{166}Ho skin patch, which was successfully used to treat squamous-cell carcinoma (SCC) in mice and humans.[12] Park et al. also reported a radioactive patch coated with ^{165}Dy, ^{166}Ho, ^{32}P, ^{192}Ir and ^{90}Y metallic particles.[10] The problem with surface coating of radionuclides is the potential to flake off. Radionuclides have also been incorporated into an adhesive agent and then coated with a protective lamination to prevent flaking.[15] Embedding the radionuclides directly in the fibers of bandages is an improvement over previously reported radioactive bandages/patches/films based on coatings.

Fibers containing nanoparticles can be prepared by a technique known as electrospinning. Fibers containing nanoparticles prepared via electrospinning can have a high surface/volume ratio, good mechanical flexibility, surface functionality and superior mechanical performance.[16] Electrospinning is a simple and effective method that uses electrostatic forces to produce nanofibrous materials with diameters ranging from a few nanometers to micrometers or greater.[17−19] Electrospinning can result in nanoparticle-embedded fibers that have nanoparticles homogeneously dispersed throughout the fiber.[20,21] The thickness of the espun mats can be varied by controlling parameters such as spinning duration, polymer concentration, applied voltage, temperature and humidity.[22] The electrospinning method is attractive because of its low cost and suitability for mass production.

In this paper, we report the preparation of a radiotherapeutic bandage containing ^{165}Ho-containing garnet (^{165}HoIG) nanoparticles incorporated in polyacrylonitrile (PAN) fibers via electrospinning. The as-synthesized ^{165}HoIG nanoparticles were dispersed in PAN polymer solutions and electrospun on aluminum foil substrates resulting in free-standing nonwoven fiber mats.

^{165}HoIG is a member of the isostructural garnet family and its general formula is $Z_3X_2Y_3O_{12}$, where the Z cations occupy the dodecahedral sites, the X cations occupy the octahedral sites and the Y cations occupy tetrahedral sites in the crystal structure, as shown in Figure S1 (Supporting Information).[23] In the case of HoIG, Ho^{3+} occupies the dodecahedral sites and Fe^{3+} occupies both the octahedral and tetrahedral sites in the structure.

Neutron-activation of the ^{165}Ho-containing bandages in a nuclear reactor resulted in radioactive bandages form the ^{166}Ho product. The ^{166}Ho-containing bandages were prepared with different amounts of radioactivity by varying the neutron-activation irradiation time and the amount of garnet nanoparticles inside the fibers. The distinct advantage of this radiotherapeutic bandage compared with the conventional radiotherapeutic patches, films and bandages is that the ^{165}Ho nanoparticles are embedded inside the fibers of the bandage. The polymer fibers are also stable after neutron-activation at a thermal neutron-flux of approximately 3.5×10^{12} neutrons/cm^2·s for at least 4 h and 100 °C. There is no leakage of radioactive material after activation, which is critical for safe handling by healthcare professionals treating skin cancer patients.

EXPERIMENTAL SECTION

Materials. Holmium(III) nitrate hexahydrate, sodium hydroxide, ethylene glycol, polyacrylonitrile (Molecular weight: 150 000 mol/g) were purchased from the Aldrich Chemical Co. Iron(III) nitrate hexahydrate was purchased from Acros Organics. Dimethylformamide (DMF) was purchased from Fisher Scientific. All reagents were used as received.

Synthesis of HoIG Nanoparticles. ^{165}HoIG nanoparticles were synthesized by modifying a reported procedure.[24] Stoichiometric mixtures (5:3) of 1 M iron(III) nitrate (5 mL) and 1 M holmium(III) nitrate (3 mL) were mixed with ethylene glycol (21 mL) at room temperature with stirring. Then 6 M NaOH (10 mL) was added dropwise to form the ^{165}HoIG nanoparticle precipitate. The product was centrifuged and washed with deionized water, then dried at 100 °C overnight. The ^{165}HoIG was annealed in air at 900 °C for 3 h.

Electrospinning of Polyacrylonitrile Polymer Solutions with ^{165}HoIG Nanoparticles (^{165}HoIG/PAN). Polyacrylonitrile (PAN) (1.0 g) was dispersed in dimethylformamide (DMF) (5 mL), with gentle heating and stirring. ^{165}HoIG nanoparticles were dispersed in DMF (5 mL) and mixed with the PAN solution at room temperature to prepare 33 and 50% w/w dispersions (Table 1). The PAN solutions containing ^{165}HoIG nanoparticles were drawn into a 12 mL syringe equipped with a 20 gauge needle and electrospun on an aluminum foil substrate wrapped around a rotating drum. The electrospinning conditions are listed in Table 1.

Neutron Activation of ^{165}HoIG and ^{165}HoIG/PAN. ^{165}HoIG nanoparticles (5 mg) and approximately 0.5 × 0.5 cm (6 mg) ^{165}Ho-containing polymer nanofibrous mats cut from both the 33% (w/w) and 50% (w/w) ^{165}HoIG/PAN were neutron-activated in a 1 MW TRIGA Mark I nuclear reactor at the Texas A&M Nuclear Science Center in a thermal neutron flux of approximately 3.5×10^{12} neutrons/cm^2·s for 0.5, 1.0, 2.0 or 4.0 h. Radioactivities were determined by quantifying the photons emitted using a gamma spectrometer. The radioactivities directly after neutron-activation are reported.

Characterization. X-ray diffraction patterns were collected on a Rigaku Ultima IV X-ray diffractometer using Cu Kα radiation. The morphology of the synthesized ^{165}HoIG nanoparticles and electrospun fibers were analyzed using scanning electron microscopy (SEM) and transmission electron microscopy (TEM). SEM analysis of Au/Pd coated samples were carried out using a Zeiss-LEO model 1530 SEM. TEM analysis was performed on JEOL 2100 analytical TEM with an accelerating voltage of 200 kV. Fourier transform infrared spectroscopy (FTIR) analysis of ^{165}HoIG nanoparticles and bandages were carried out using a Nicolet 380 spectrometer equipped with an attenuated total reflectance (ATR) attachment. Thermogravimetric analysis (TGA) was performed using TA Instruments SDT Q600. Inductively coupled plasma-mass spectrometry (ICP-MS) was performed to determine the ^{165}Ho content in ^{165}HoIG using NexION 300D from PerkinElmer. γ-Radiation of neutron activated samples was measured using a Canberra Industries HPGe GC3518 instrument.

RESULTS AND DISCUSSION

^{165}HoIG Nanoparticles. Figure 1 shows the PXRD patterns for the as-synthesized ^{165}HoIG nanoparticles. The phase matches well with $Fe_5Ho_3O_{12}$ (JCPDS 00-023-0282). The crystallite sizes were calculated from the PXRD line broadening of the 420 reflection using the Scherrer equation, $D_{hkl} = k\lambda/B \cos\theta$, where D_{hkl} is the particle size in nm, k is a constant (shape factor) with a value of 0.9, B is the width of half-maximum and λ is the wavelength of the X-rays. The D_{hkl} value of ^{165}HoIG is about 52 nm.

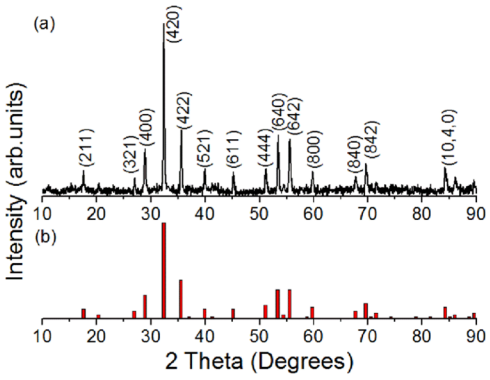

Figure 1. PXRD pattern of (a) ^{165}HoIG powder and (b) $Fe_5Ho_3O_{12}$; JCPDS 00-023-0282.

TEM images of the as synthesized ^{165}HoIG nanoparticles are shown in Figure 2. The nanoparticles generally exhibited a

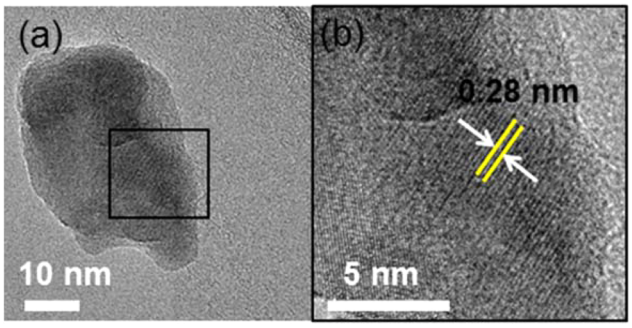

Figure 2. (a) TEM (b) HRTEM images of as-synthesized ^{165}HoIG nanoparticle.

rounded irregular shaped morphology. The length of ^{165}HoIG is 55 nm and the width is 28 nm. The interplanar distance of ^{165}HoIG is 0.28 nm (Figure 2 (b), which corresponds to the (420) plane is d = 0.278 nm in Figure 1. Using ICP-MS, the ^{165}HoIG was determined to contain 55.6% (w/w) Holmium.

Electrospinning of PAN Containing HoIG Nanoparticles. Figure S2 (Supporting Information) shows the digital image of the electrospun fiber mat with 33% (w/w) ^{165}HoIG loading. SEM images of the electrospun fiber mats with different ^{165}HoIG nanoparticle loadings are shown in Figure 3a-1,a-2.

As shown in the histogram, 90% of fibers are below 300 nm. The average diameters of nanofibers are 174 ± 56 nm and 208 ± 54 nm when the ^{165}HoIG loadings were 33% and 50% (w/w). The increase in the fiber diameter with increasing ^{165}HoIG content may reflect the size of the garnet nanoparticles as well as agglomeration.[24,25]

The TEM images of the electrospun PAN fiber with 33% (w/w) of HoIG nanoparticles is shown in Figure 4. Figure 4a-2 shows the 420 lattice planes of the ^{165}HoIG nanoparticles that are inside the PAN fibers with the d spacing value of 0.28 nm. This confirms the presence of ^{165}HoIG nanoparticles inside nanofibers.

Figure S3 (Supporting Information) shows the comparison of the FTIR spectra of ^{165}HoIG powder, pure PAN and electrospun ^{165}HoIG/PAN fibers. Peaks around 548 and 584 cm^{-1} (Figure S3c, Supporting Information) are due to the metal−oxygen vibrations of ^{165}HoIG.[26] FTIR spectrum of PAN

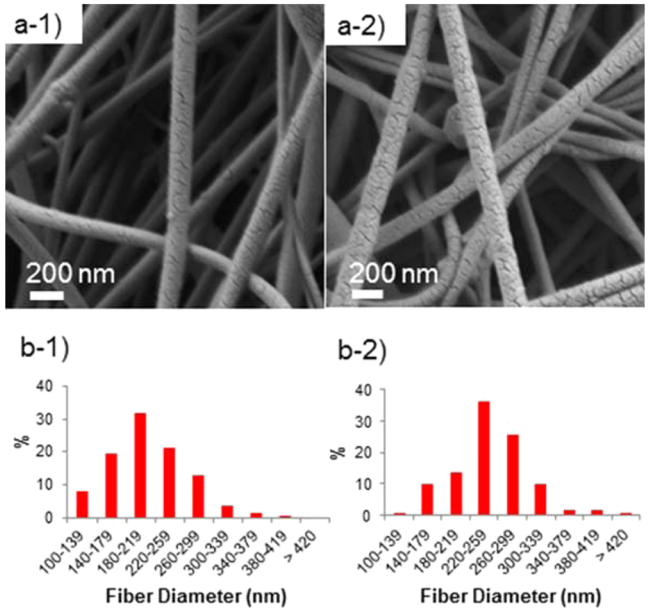

Figure 3. SEM images and fiber diameter distributions of (a-1, b-1) 33% (w/w) HoIG loaded- and (a-2, b-2) 50% (w/w) HoIG loaded-electrospun fiber mats (using 30 images).

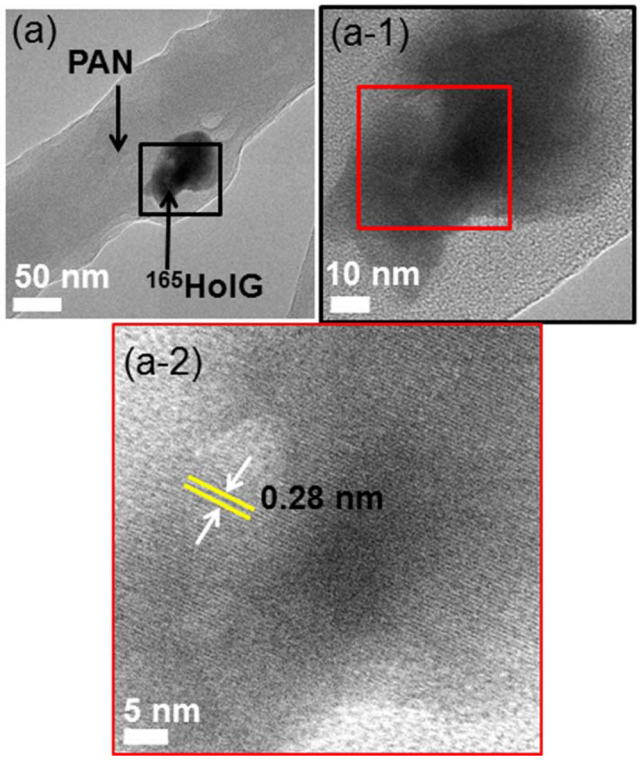

Figure 4. (a), (a-1) TEM (a-2) HRTEM images of electrospun 33% (w/w) ^{165}HoIG/PAN fiber.

composite with ^{165}HoIG particles (Figure S3b, Supporting Information) shows a blue shift as compared to the FTIR spectrum of ^{165}HoIG. The slight shifts in the Fe−O bond of magnetic particles have been reported for magnetic nanoparticles encapsulated in polyacrylonitrile,[27] wrapped with polyethylene glycol and polyvinyl pyrrolidone[28] and coated with 3-aminopropyltriethoxysilane.[29] This is due to the polymer binding to the nanoparticles and some physical interaction on

the surface of magnetic nanoparticles.[28] Therefore, similar explanation can be used for the blue shift of metal−oxygen vibration in ^{165}HoIG/PAN spectrum. There is a good interaction between radioactive nuclides and PAN inside the fibers and radioactive nanoparticles will not leach from the bandage. To verify this, radiotherapeutic bandages (before and after neutron activation) were soaked in simulated body fluid (SBF) and DI water for 4 and 8 h and samples from SBF and water were analyzed using TEM to check whether there is any loss of the embedded nanoparticles from the PAN fibers. There were no free nanoparticles detected in the samples. These results confirm that radioactive particles do not leach out from the radiotherapeutic bandage. The XRD patterns of the electrospun fibers with 33% (w/w) loading of HoIG nanoparticles shown in Figure S4 (Supporting Information) further confirm the presence of ^{165}HoIG nanoparticles in nanofibers.

Neutron-Activation of ^{165}HoIG Nanoparticles and ^{165}HoIG/PAN Bandages. ^{165}HoIG and rectangles of ^{165}HoIG/PAN were neutron-activated for 0.5, 1, 2 and 4 h. Radioactivities of 56.8, 330.7, 833.8 and 1633.6 μCi/mg were obtained for ^{166}HoIG nanoparticles, after approximately 0.5, 1, 2 and 4 h neutron-activation, respectively. From these data, we can calculate that ^{166}HoIG nanoparticles contain 57.8 ± 26.2% (w/w) ^{166}Ho, which corroborates the ICP-MS data.

It is critical for the ^{166}HoIG/PAN bandage to emit radiation uniformly during therapy; thus, four rectangular pieces were cut from a 33% ^{165}HoIG/PAN in four different locations (Figure S5a, Supporting Information) and neutron-activated for 0.5 h. The same was done for the 50% HoIG/PAN bandage (Figure S5b, Supporting Information). After neutron-activation, the radioactivities were measured and ^{166}Ho content determined; 17.1 ± 0.7% and 22.7 ± 1.9% of ^{166}Ho was contained in electrospun fibers with 33% (w/w) HoIG and 50% (w/w) HoIG, respectively (Figure S5, Supporting Information). This is consistent with a uniform dispersion of ^{166}HoIG throughout the bandage after electrospinning, as well as efficient loading of HoIG into the bandage.

Radioactivities of 48.1, 101.1, 479.2 and 650.3 μCi/mg were produced for 33% HoIG/PAN, and 63.7, 163.3, 300.0 and 854.7 μCi/mg for 50% HoIG/PAN, after 0.5, 1, 2 and 4 h neutron-activation, respectively. Thus, radioactivities of 6.420×10^2, 1.675×10^3, 1.917×10^4 and 2.016×10^4 μCi/cm^2 were produced for 33% HoIG/PAN bandages, and 1.411×10^3, 6.532×10^3, 4.501×10^3 and 2.607×10^4 μCi/cm^2 were produced for 50% HoIG/PAN bandages.

Radioactivity can be calculated using the following formula:

$$A = nfs(1 - e^{-\lambda T})e^{-\lambda t}$$

where A is the radioactivity produced (Bq/mg, which is 2.7×10^{-11} Ci/mg), n is the number of atoms per mg, f is neutron flux density (n/cm^2·s), s is the thermal neutron capture cross section (cm^2), λ is the decay constant ($0.693/t_{1/2}$), T is the irradiation time and t the is decay time. Here, nfs is a constant, and immediately after neutron-activation, t is 0. Thus, A should be proportional to $1 - e^{-\lambda T}$.

We here plot radioactivity (A) in μCi/mg against $1 - e^{-\lambda T}$ (Figure 5). Least-squares linear fits give R^2 values of 0.93, 0.96 and 0.98 for the 33 and 50% HoIG/PAN and HoIG data sets, respectively. A ^{32}P radioactive patch, ^{188}Re-labeled nitrocellulose paper and ^{166}Ho patch have been reported with radioactivities of 37 MBq/cm^2 (1000 μCi/cm^2), 74 MBq/cm^2 (2000 μCi/cm^2) and 4−6 mCi for a film 1 cm in diameter

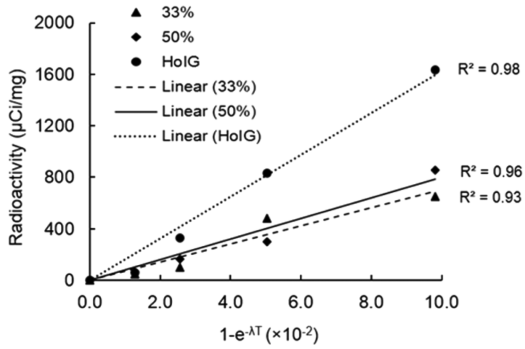

Figure 5. Radioactivity of HoIG nanoparticles, 33% and 50% (w/w) HoIG bandages plotted against $(1 - e^{-\lambda T})$.

(955−1432 μCi/cm^2), respectively.[15,30,13] ^{90}Y ethylene glycol methacrylate phosphate patches have also been developed for brachytherapy applications, with a radioactivity of 185 MBq/cm^2 (5000 μCi/cm^2).[31] The radioactivities obtained for our ^{166}HoIG-containing radioactive bandages are comparable to these values, and, thus, therapeutic activities can be achieved. Furthermore, due to the demonstrated stability upon neutron-activation, the HoIG/PAN bandage can be irradiated for longer times, resulting in higher radioactivities.

Total doses of 35 to 70 Gy are used in radiation therapy.[12] Previously, a holmium 166 skin patch was reported.[12] In this case, the patch was made by sticking the holmium nanoparticles on an adhesive tape and then coated by a polyethylene microfilm. 5 mm size patches were tested on mice with chemically induced skin tumors (22.2−72.15 MBq (0.6−1.95 mCi)) and human patients with squamous cell carcinoma (273.8−999 MBq (74−27 mCi)).[12] After the radioactive patch was applied on the tumor surface, the tumors decreased in size for squamous cell carcinoma. The total absorbed radiation dose in each tumor was estimated to be 50 Gy for the human and 42−45 Gy for the animal.[12] Thus, 6750 μCi/cm^2 might be considered the minimum radioactivity needed for human patients. A therapeutic effect is expected for the HoIG/PAN bandages because the radioactivity is comparable to the previously reported radioactive patch.

Figure 6 shows the TGA curve of ^{165}HoIG containing electrospun polymer nanofibrous mat (33% (w/w)).

The ^{165}Ho/PAN fiber nanocomposite is thermally stable until the temperature reaches 292 °C. A sharp weight loss around 290 °C is mainly due to the formation of the ring

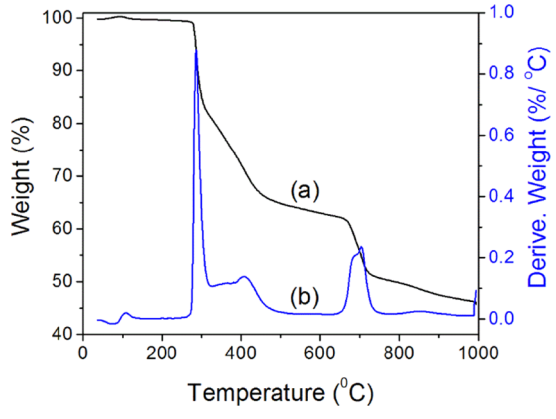

Figure 6. (a) TGA (b) DTA curve of HoIG/PAN bandage.

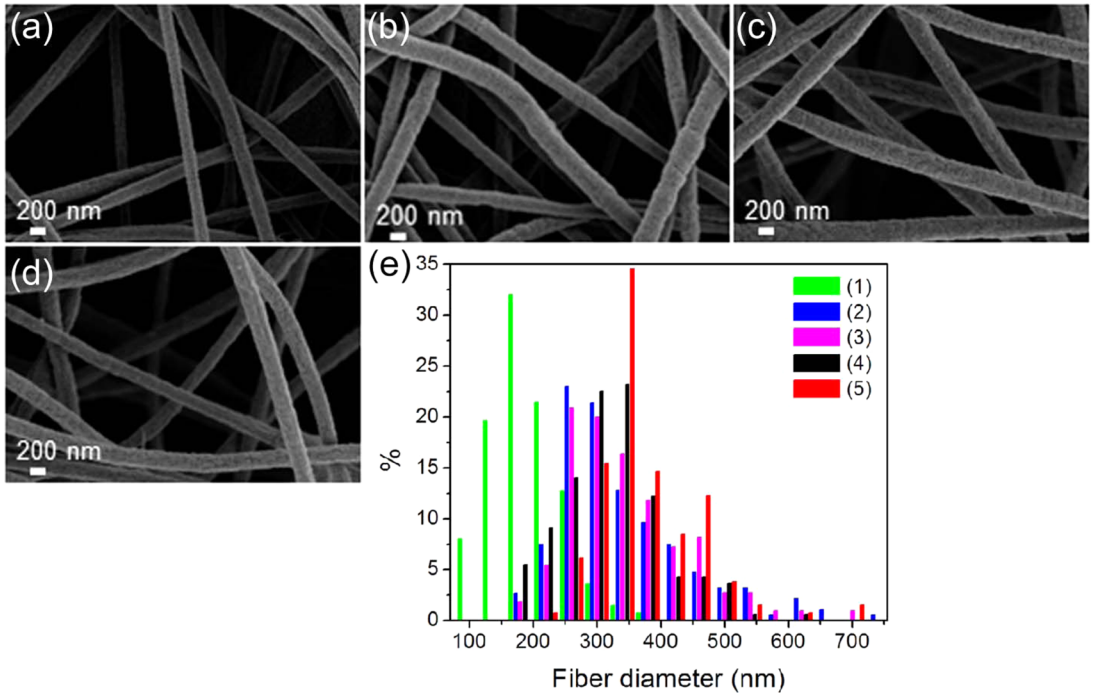

Figure 7. SEM images and fiber diameter distributions of 33% (w/w) HoIG loaded bandages before (e-1) and after neutron activated for (a) (e-2), 0.5 h; (b) (e-3), 1.0 h; (c) (e-4), 2.0 h; (d) (e-5), 4.0 h (using 25 images).

compounds from the CN groups.[32] This process is accompanied by degradative loss of H_2, NH_3, and HCN.[33] Internal γ heating of the samples inside the nuclear reactor raises the temperature of the samples. TGA study shows that ^{165}HoIG/PAN bandages are thermally stable up to 290 °C; consistent with the radiotherapeutic ^{165}HoIG/PAN bandages being stable after neutron-activation.

In Figure S6 (Supporting Information), the bandages are shown before and after neutron-activation; the macroscopic appearance of the material looks similar before and after neutron-activation. However, the SEM images of neutron activated fibers shown in Figures 7 and S7 (Supporting Information) show an increase in diameter. The average diameter of nanofibers are 302 ± 79, 320 ± 94, 323 ± 94 and 353 ± 79 nm (Figure 7) when the HoIG loadings (w/w) are 33% and 317 ± 86, 339 ± 70, 358 ± 84 and 360 ± 88 nm (Figure S7, Supporting Information) when the HoIG loadings (w/w) are 50% for 0.5, 1.0, 2.0 and 4.0 h neutron activated bandages, respectively. Thus, there is an increase in the fiber diameter of neutron activated bandages compared to the non-neutron activated bandages (Figures 7e and S7e, Supporting Information).

There have been a few reports of the effect of neutron irradiation on carbon−carbon composites and dimension changes in carbon fibers.[34,35] Carbon fibers made of polyacrylonitryle (PAN) demonstrated in a carbon matrix anisotropic size deformation upon neutron irradiation: shrinkage along the fiber axis and swelling in the perpendicular direction.[34,36] A control experiment was conducted by heating the electropun PAN fibers and 33% HoIG/PAN bandages at different temperatures. These fiber mats were prepared using the same conditions as listed in Table 1. Figure 8 shows the SEM images of the heated 33% HoIG/PAN bandages at different temperatures. The average diameter of fibers are 174 ± 56, 214 ± 47, 264 ± 72 and 291 ± 58 nm for nonheated fibers and 100 °C, 150 and 200 °C heated fibers, respectively.

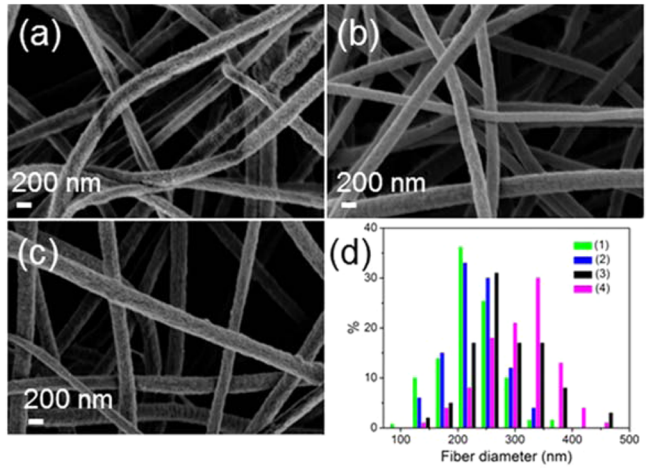

Figure 8. SEM images and fiber diameter distributions of 33% (w/w) HoIG loaded bandages before heated (d-1) and after heated at (a) (d-2), 100 °C; (b) (d-3), 150 °C; (c) (d-4), 200 °C.

Figure S8 (Supporting Information) shows the SEM images of heated fibers of PAN bandages without HoIG at different temperatures and the average fiber diameter of fibers are 114 ± 29, 245 ± 97, 332 ± 92 and 349 ± 87 nm for nonheated fibers and 100 °C, 150 and 200 °C heated fibers, respectively. There is an increase in the fiber diameter of PAN and 33% HoIG/PAN fibers due to the heat treatments. Because the HoIG is not responsible for the increase, residual solvent may be the cause. TGA of the 33% HoIG/PAN (Figure 6) and PAN (Figure S9, Supporting Information) bandages show an initial 2% weight lost around 100 °C due to the removal of residual solvent. Thus, the HoIG/PAN fibers must be heated to at least 100 °C during neutron activation.

This study demonstrates ^{166}Ho containing bandages with different amounts of radioactivity can be prepared by varying the neutron-activation time and the amount of neutron-activatable nuclide incorporated. Preparing and handling large amounts of hazardous, highly radioactive materials with short half-lives can be cumbersome and, thus, is here avoided using neutron-activatable ^{165}Ho.

The mechanistic pathways of cancer cell death due to the radiation therapy has been widely reported and involves the penetration of β-energy through skin tumors and direct/indirect effects of radiation.[37] Direct effect radiation can directly interact with cellular DNA and cause damage DNA in the cancer cells.[37] The indirect DNA damage caused by the free radicals is derived from the ionization or excitation of the water component of the cancer cells.[37] The β-energy of ^{166}Ho should be sufficient to damage DNA in cancer cells just beneath the outermost layer of the epidermis, and it is expected that the stratum corneum will protect any normal skin surrounding the tumor lesion from radiation damage. Thus, this approach could help patients achieve optimized cosmetic and/or functional outcomes without the use of specialized instrumentation or facilities. It is envisioned that a lead wrap could be placed around the bandage during treatment while sitting in a physician's office.

The next stage of this research is to optimize the radiotherapeutic bandages using human squamous cell carcinoma (SCC) cell lines and evaluate the efficacy of the radiotherapeutic bandages in a human SCC xenograft mouse model. This follows the approach of other research groups studying radioactive paper, films and adhesive tapes with radionuclide coatings on the surface in clinical and animal trials.[10−12] We here developed a novel bandage that should be more safe to handle in clinical settings. Additionally, tthe radiotherapeutic activity can be altered as desired. It is anticipated that therapeutic comparable to previous human and animal studies can be easily obtained by changing the size of the bandage and the neutron activation time.

CONCLUSIONS

Novel radiotherapeutic bandages were successfully prepared for the first time via electrospinning, a simple and economic approach that uses electrostatic forces to produce nanofibrous materials. Specifically, ^{165}Ho-containing nanoparticles were homogeneously incorporated into electrospun polymer nanofibrous mats, and then made radioactive via neutron-activation, i.e., ^{165}Ho to ^{166}Ho. The bandages are stable after neutron-activation at a thermal neutron-flux of approximately 3.5×10^{12} neutrons/cm^2·s for at least 4 h and 100 °C. The bandage was shown to be quite pliable; thus, it can conform to a cancer site and treat a specific covered area without leaching the nanoparticles. Different amounts of radioactivity can be produced by changing the amount of ^{165}HoIG nanoparticles inside the bandage and the duration of neutron-activation. Also, the radioactive bandage can easily be manipulated to irradiate only the lesion site, via cutting to specific shapes and sizes prior to neutron-activation. In this way, the possibility of death of normal cells can be avoided. Moreover, multiple sites can be treated simultaneously using these radioactive bandages. A further advantage of this work is that it can be easily scaled-up and could be rapidly moved to the clinic.

ASSOCIATED CONTENT

Supporting Information

Crystal structure (cubic, *Ia3d*) of garnet calculated using the crystallographic data in ref 23, Digital image of 33% (w/w) HoIG/PAN electrospun fiber mat; FTIR spectra of PAN, ^{165}HoIG/PAN fiber and ^{165}HoIG powder; PXRD pattern of ^{165}HoIG powder and electrospun fibers with 33% (w/w) ^{165}HoIG; diagrams showing homogeneity of 33% (w/w) ^{166}Ho-containing electrospun polymer nanofibrous mats; 33% (w/w) ^{166}Ho-containing electrospun PAN mats before (control) and after neutron-activation for 0.5, 1.0, 2.0 and 4.0 h in a thermal neutron flux of approximately 3.5×10^{12} n/cm^2·s in a 1 MW nuclear reactor; SEM images and fiber diameter distributions of 50% (w/w) HoIG-loaded bandages before and after neutron-activation for 0.5, 1.0, 2.0 and 4.0 h (using 25 images), SEM images and fiber diameter distributions of PAN bandages before heated and after heated at 100, 150 and 200 °C; TGA and DTA curve of electrospun PAN fibers. This material is available free of charge via the Internet at http://pubs.acs.org.

AUTHOR INFORMATION

Corresponding Authors

*A. J. Di Pasqua. E-mail: Anthony.DiPasqua@unthsc.edu. Tel: (817) 735-2144. Fax: (817) 735-2603.
*K. J. Balkus, Jr. E-mail: balkus@utdallas.edu.

Notes

The authors declare no competing financial interest.

ACKNOWLEDGMENTS

We thank Ms. Ashley Booth at the Texas A&M Nuclear Science Center for her help. This work was financial supported by the Texas Medical Research Collaborative (TexasMRC).

REFERENCES

(1) Robinson, J. K. Sun Exposure, Sun Protection, and Vitamin D. *JAMA, J. Am. Med. Assoc.* **2005**, *294*, 1541−1543.
(2) Chinn, D. M.; Chow, S.; Kim, Y. H.; Hoppe, R. T. Total Skin Electron Beam Therapy with or without Adjuvant Topical Nitrogen Mustard or Nitrogen Mustard Alone as Initial Treatment of T2 and T3 Mycosis Fungoides. *Int. J. Radiat. Oncol., Biol., Phys.* **1999**, *43*, 951−958.
(3) Wilder, R. B.; Kittelson, J. M.; Shimm, D. S. Basal Cell Carcinoma Treated with Radiation Therapy. *Cancer* **1991**, *68*, 2134−2137.
(4) Hofmann, B.; Fischer, C. O.; Lawaczeck, R.; Platzek, J.; Semmler, W. Gadolinium Neutron Capture Therapy (GdNCT) of Melanoma Cells and Solid Tumors with the Magnetic Resonance Imaging Contrast Agent Gadobutrol. *Invest. Radiol.* **1999**, *34*, 126−133.
(5) Smith, G. L.; Jiang, J.; Buchholz, T. A.; Xu, Y.; Hoffman, K. E.; Giordano, S. H.; Hunt, K. K.; Smith, B. D. Benefit of Adjuvant Brachytherapy Versus External Beam Radiation for Early Breast Cancer: Impact of Patient Stratification on Breast Preservation. *Int. J. Radiat. Oncol., Biol., Phys.* **2014**, *88*, 274−284.
(6) Bult, W.; Kroeze, S. G. C.; Elschot, M.; Seevinck, P. R.; Beekman, F. J.; de Jong, H. W. A. M.; Uges, D. R. A.; Kosterink, J. G. W.; Luijten, P. R.; Hennink, W. E.; Van het Schip, A. D.; Bosch, J. L. H. R.; Nijsen, J. F. W.; Jans, J. J. M. Intratumoral Administration of Holmium-166 Acetylacetonate Microspheres: Antitumor Efficacy and Feasibility of Multimodality Imaging in Renal Cancer. *PLoS One* **2013**, *8*, e52178.
(7) Gasser, S.; Raulet, D. The DNA Damage Response, Immunity and Cancer. *Semin. Cancer Biol.* **2006**, *16*, 344−347.
(8) Di Pasqua, A. J.; Yuan, H.; Chung, Y.; Kim, J. K.; Huckle, J. E.; Li, C.; Sadgrove, M.; Tran, T. H.; Jay, M.; Lu, X. Neutron-Activatable Holmium-Containing Mesoporous Silica Nanoparticles as a Potential

Radionuclide Therapeutic Agent for Ovarian Cancer. *J. Nucl. Med.* **2013**, *54*, 111−116.
(9) Memon, K.; Lewandowski, R. J.; Riaz, A.; Salem, R. Yttrium 90 Microspheres for the Treatment of Hepatocellular Carcinoma. *Recent Results Cancer Res.* **2013**, *190*, 207−224.
(10) Park, K.-B.; Kim, J.-R.; Lee, J.-D. Radioactive Patch for Curing a Skin Disease and Manufacturing Method Thereof. European PatentEP 0730872 A1, Sep 11, 1996.
(11) Chung, Y. L.; Lee, J. D.; Bang, D.; Lee, J. B.; Park, K. B.; Lee, M.-G. Treatment of Bowen's Disease with a Specially Designed Radioactive Skin Patch. *Eur. J. Nucl. Med.* **2000**, *27*, 842−846.
(12) Lee, J. D.; Park, K. K.; Lee, M. G.; Kim, E. H.; Rhim, K. J.; Lee, J. T.; Yoo, H. S.; Kim, Y. M.; Park, K. B.; Kim, J. R. Radionuclide Therapy of Skin Cancers and Bowen's Disease Using a Specially Designed Skin Patch. *J. Nucl. Med.* **1997**, *38*, 697−702.
(13) Jeong, J. M.; Lee, Y. J.; Kim, E.-H.; Chang, Y. S.; Kim, Y. J.; Son, M.; Lee, D. S.; Chung, J.-K.; Lee, M. C. Preparation of ^{188}Re-Labeled Paper for Treating Skin Cancer. *Appl. Radiat. Isot.* **2003**, *58*, 551−555.
(14) Pandey, U.; Sarma, H. D.; Ingle, A. D.; Kulloli, B. S.; Samuel, G.; Venkatesh, M. Radioactive Skin Bandages Incorporating ^{32}P for Treatment of Superficial Tumors. *Cancer Biother.Radiopharm.* **2006**, *21*, 257−262.
(15) Park, K. B.; Kim, J.-R.; Lee, J.-D. Radioactive Patch/Film and Process for Preparation Thereof. U.S. Patent US 5871708 A, Feb 16, 1999.
(16) Huang, Z.-M.; Zhang, Y. Z.; Kotaki, M.; Ramakrishna, S. A Review on Polymer Nanofibers by Electrospinning and Their Applications in Nanocomposites. *Compos. Sci. Technol.* **2003**, *63*, 2223−2253.
(17) Sill, T. J.; Von Recum, H. A. Electrospinning: Applications in Drug Delivery and Tissue Engineering. *Biomaterials* **2008**, *29*, 1989−2006.
(18) Agarwal, S.; Wendorff, J. H.; Greiner, A. Use of Electrospinning Technique for Biomedical Applications. *Polymer* **2008**, *49*, 5603−5621.
(19) Lee, K. Y.; Jeong, L.; Kang, Y. O.; Lee, S. J.; Park, W. H. Electrospinning of Polysaccharides for Regenerative Medicine. *Adv. Drug Delivery Rev.* **2009**, *61*, 1020−1032.
(20) Anka, F. H.; Perera, S. D.; Ratanatawanate, C.; Balkus, K. J., Jr. Polyacrylonitrile Gold Nanoparticle Composite Electrospun Fibers Prepared by In Situ Photoreduction. *Mater. Lett.* **2012**, *75*, 12−15.
(21) Song, W.; Markel, D. C.; Wang, S.; Shi, T.; Mao, G.; Ren, W. Electrospun Polyvinyl Alcohol-Collagen-Hydroxyapatite Nanofibers: A Biomimetic Extracellular Matrix for Osteoblastic Cells. *Nanotechnology* **2012**, *23*, 115101−115115.
(22) Lu, P.; Ding, B. Applications of Electrospun Fibers. *Recent Pat. Nanotechnol.* **2008**, *2*, 169−182.
(23) Komori, T.; Sakakura, T.; Takenaka, Y.; Tanaka, K.; Okuda, T. Trineodymium(III) Pentairon(III) Dodecaoxide, $Nd_3Fe_5O_{12}$. *Acta Crystallogr., Sect. E: Struct. Rep. Online* **2009**, *65*, 72.
(24) Munaweera, I.; Aliev, A.; Balkus, K. J., Jr. Electrospun Cellulose Acetate-Garnet Nanocomposite Magnetic Fibers for Bioseparations. *ACS Appl. Mater. Interfaces* **2014**, *6*, 244−251.
(25) Hassan, M. I.; Sultana, N.; Hamdan, S. Bioactivity Assessment of Poly(ε-caprolactone)/Hydroxyapatite Electrospun Fibers for Bone Tissue Engineering Application. *J. Nanomater.* **2014**, *2014*, 6.
(26) Veitch, C. D. Synthesis of Polycrystalline Yttrium Iron Garnet and Yttrium Aluminum Garnet from Organic Precursors. *J. Mater. Sci.* **1991**, *26*, 6527−6532.
(27) Khan, A.; El-Toni, A. M.; Alsalhi, M.; Aldwayyan, A. S.; Alhoshan, M. Preparation of Magnetic Polyacrylonitrile Core−Shell Nanospheres by the Miniemulsion Polymerization Method. *Mater. Lett.* **2012**, *76*, 141−143.
(28) Kumar, S. R.; Marianna, L.; Gianni, S.; Nathanael, A. J.; Hong, S. I.; Oh, T. H.; Mangalaraj, D.; Viswanathan, C.; Ponpandian, N. Hydrophilic Polymer Coated Monodispersed Fe_3O_4 Nanostructures and Their Cytotoxicity. *Mater. Res. Express* **2014**, *1*, 015015.
(29) Ma, M.; Zhang, Y.; Yu, W.; Shen, H. Y.; Zhang, H. Q.; Gu, N. Preparation and Characterization of Magnetite Nanoparticles Coated by Amino Silane. *Colloids Surf., A* **2003**, *212*, 219−226.
(30) Saxena, S. K.; Kumar, Y.; Pandey, U.; Shinde, S. N.; Muthe, K. P.; Venkatesh, M.; Dash, A. A Facile, Viable Approach Toward the Preparation of 32P Patches for the Treatment of Skin Cancer. *Cancer Biother.Radiopharm.* **2011**, *26*, 665−670.
(31) Saxena, S. K.; Pandey, A. K.; Tandon, P.; Chakravarty, R.; Reddy, A. V. R.; Dash, A.; Venkatesh, M. A Novel Approach to Prepare 90Y−EGMP Patches for Superficial Brachytherapy. *Appl. Radiat. Isot.* **2009**, *67*, 1416−1420.
(32) Zhu, J.; Wei, S.; Rutman, D.; Haldolaarachchige, N.; Young, D. P.; Guo, Z. Magnetic Polyacrylonitrile-Fe@FeO Nanocomposite Fibers - Electrospinning, Stabilization and Carbonization. *Polymer* **2011**, *52*, 2947−2955.
(33) Zhang, D.; Chung, R.; Karki, A. B.; Li, F.; Young, D. P.; Guo, Z. Magnetic and Magnetoresistance Behaviors of Solvent Extracted Particulate Iron/Polyacrylonitrile Nanocomposites. *J. Phys. Chem. C* **2010**, *114*, 212−219.
(34) Burchell, T. D.; Eatherly, W. P.; Robbins, J. M.; Strizak, J. P. The Effect of Neutron Irradiation on the Structure and Properties of Carbon-Carbon Composite Materials. *J. Nucl. Mater.* **1992**, *191−194*, 295−299.
(35) Burchell, T. D. Irradiation-Induced Structure and Property Changes in Tokamak Plasma-Facing, Carbon-Carbon Composites. *Int. SAMPE Symp. Exhib.* **1994**, *39*, 2423−2436.
(36) Blazewicz, S.; Blocki, J.; Chlopek, J.; Goolewski, J.; Michalowski, J.; Pakonski, K.; Piekarczyk, J.; Stodulski, M. Thin C/C Composite Shells for High Energy Physics: Manufacture and Properties. *Carbon* **1996**, *34*, 1393−1399.
(37) Baskar, R.; Lee, K. A.; Richard, Y.; Yeoh, K. W. Cancer and Radiation Therapy: Current Advances and Future Directions. *Int. J. Med. Sci.* **2012**, *9*, 193−199.